Chemistry and Materials

The Center for Science Innovation

Research Article

Chem. Mater. 1 (3) 2022, 88-92

The Effect of Deposition Potential on the Electrodeposition of Platinum Nanoparticles for Ethanol Electrooxidation

Amelia Sabella[1,*], Reyhan Syifa[1], Nandita Annisa Dwiyana[2]

[1]Department of Chemistry, Faculty of Mathematics and Natural Sciences, Universitas Negeri Jakarta, Jl. Rawamangun Muka, Jakarta 13220, Indonesia

[2]English Literature, Faculty of English Department, Universitas Pamulang, Jl. Surya Kencana Pamulang, Kota Tangerang Selatan 15417, Indonesia

*Corresponding author: ameliasabella18@gmail.com

Received
6 October 2022

Received in revised form
28 October 2022

Accepted
7 November 2022

Published online
15 November 2022

DOI
https://doi.org/10.56425/cma.v1i3.46

Abstract

Platinum (Pt) nanoparticles were successfully prepared using square wave pulse deposition technique by varying the upper potential. The X-ray energy dispersive spectrum pattern confirmed the formation of Pt nanoparticles on the fluorine-doped tin oxide coated glass substrate. The results of scanning electron microscopy showed that the potential of 0.60 V was able to produced a large number of Pt particles with a unique morphology. The ethanol electrooxidation test conducted using cyclic voltammetry showed that $Pt_{0.60V}$ has the lowest charge transfer resistance value showing high catalytic activity which could be associated to the increase of particle number and its active sites that activated the redox reactions in the system.

Keywords: Pt, electrodeposition, ethanol electrooxidation

1. Introduction

In recent years, direct ethanol fuel cells (DEFCs) and direct methanol fuel cells (DMFCs) have high possibility to replace conventional fossil fuels and reduce energy crisis and green house gas emissions. Compared to DMFCs, DEFCs demonstrates remarkable advantages, such as safer and easier to store and transport as well as lower costs for producing and handling ethanol fuel [1,2]. Moreover, ethanol significantly has higher energy density than methanol (6.28 kWh/L for ethanol vs 4.82 kWh/L for methanol) [3]. Demirci and M. Li et al., also reported that ethanol has a high specific energy which is 8.01 $kWh \cdot kg^{-1}$ comparable to gasoline [4,5].

In DEFCs, an active electrocatalyst with high activity was required to break the C-C bond in ethanol [6] so the complete ethanol oxidation occured at lower overpotential. These reactions aimed to improve cell performace, ethanol conversion rate, and fuel efficiency [7]. Platinum (Pt), has been reported, as an electrocatalyst that provides a large number of active coordination sites and relatively high selectivity to promoted inter-carbon alcohol bonds cleavage [8]. Pt catalyst activity can also be increased by modifying the structure during synthesis [9]. One of the method that can be used to modify the structure of Pt is electrodeposition. This method commonly used due to its simple process, low cost, and the ability to regulate the growth of the material to be synthesized [10,11]. The electrodeposition technique has several controllable parameters including the concentration of the precursor, the supporting electrolyte, the time, and the deposition potential. According to the previous studies, the potential used in electrodeposition process can affect the morphology and electrochemical properties [12]. In this study, Pt nanoparticles was synthesized through electrodeposition by varying the potential, thus it was expected the morphology, impedance, and catalytic performance of ethanol electrodeposition can be increased.

2. Materials and Method

The method used to synthesize Pt nanoparticles is a square wave pulse deposition carried out at room temperature in a salt solution of K_2PtCl_6 1 mM and a

supporting electrolyte of H_2SO_4 1 M. The materials used for this study consisted of K_2PtCl_6, H_2SO_4, KCl, C_2H_5OH 96%, and NaOH. All the materials were purchased from PT Merck Indonesia. While for the substrate used fluorine-doped tin oxide (FTO) coated glass 10 ohm/sq purchased from NSG Pilkington. The electrodeposition process is controlled by eDAQ ER466 which is connected to three electrode systems: Pt wire as a counter electrode, Ag/AgCl (3 M) as a reference electrode, and FTO as a working electrode. The electro-deposition of Pt nanoparticles occured at a lower potential -0.5 V and different upper potentials of 0.30, 0.60, and 1.00 V for 10 minutes deposition time. After the electro-deposition process is completed, the sample is rinsed with aquadest and dried. The samples were labelled as $Pt_{0.30V}$, $Pt_{0.60V}$, and $Pt_{1.00V}$, respectively. The synthesized samples were subsequently characterized by X-ray Diffraction (XRD) (SmartLab Rigaku Co. Ltd., Japan) using the Cu-Kα radiation source to identify the presence of a Pt nanoparticle phase in the sample, scanning electron microscopy was connected with energy dispersive X-ray (SEM-EDX) (FEI Inspect F50) to observe the morphology and elemental composition of the sample, electrochemical impedance spectroscopy (EIS) (Corrtest CS310) at a frequency of 50 kHz to 0.1 Hz in a 0.5 M KCl solution to determine the electrochemical properties of the sample. Ethanol electrooxidation activity in sample was elucidated by cyclic voltammetry (CV) in 0.1 M NaOH and 1 M ethanol with potential range appproximately around -0.75 to 0.75 V and scan rate 25 mV/s.

3. Results and Discussion

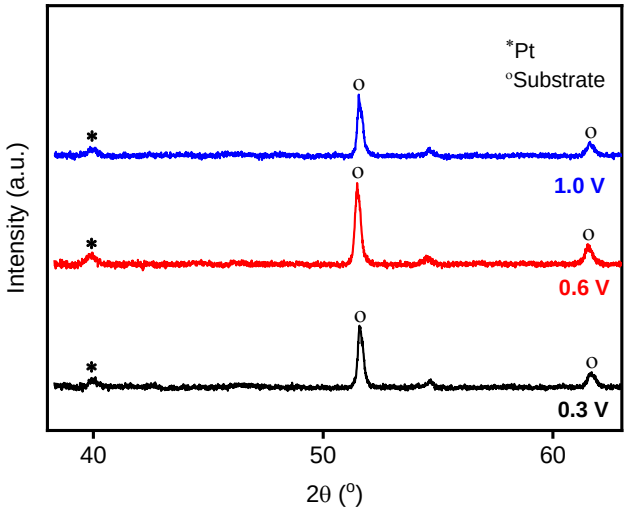

Figure 1. XRD pattern of Pt nanoparticles with different upper potential.

XRD results of Pt samples are shown in Fig. 1. All diffractograms confirmed the formation of Pt nanoparticles on the FTO surface. According to the observed data, the peak that apperead at 2Θ = 39.92° came from Pt metal [13-15].

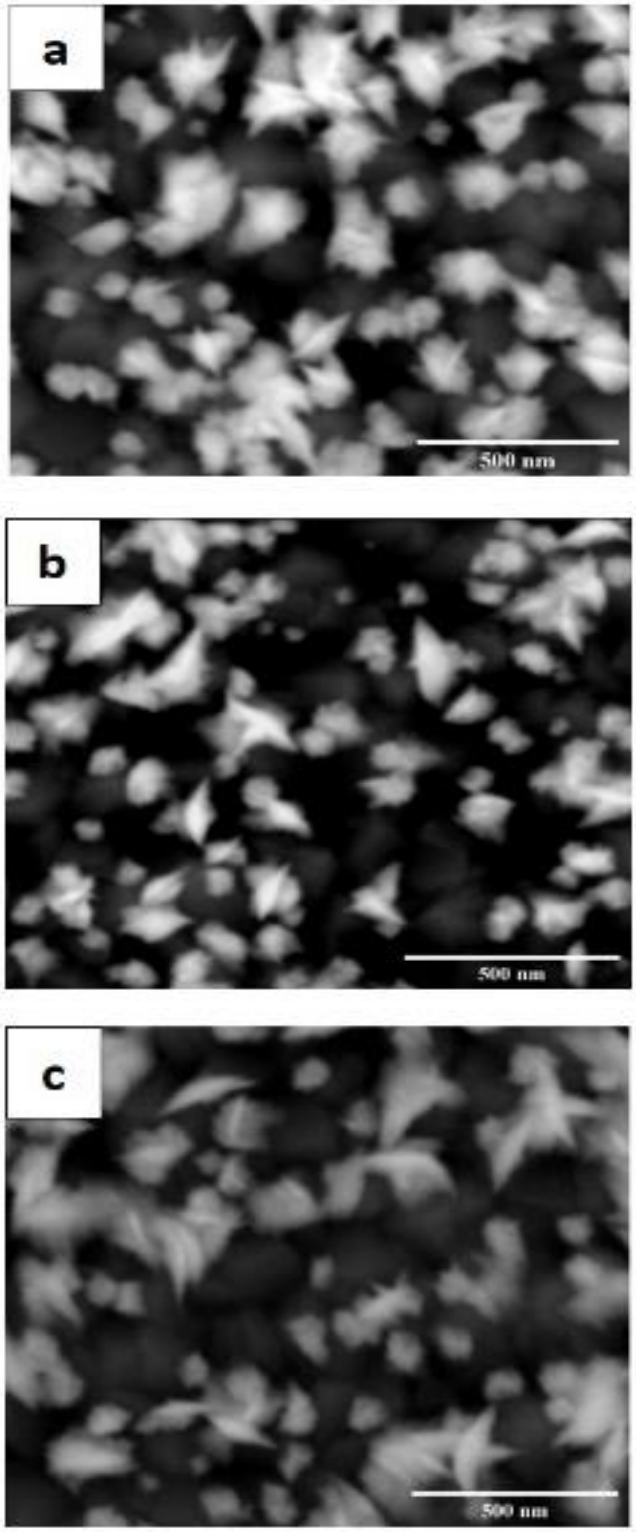

Figure 2. Micrographs of synthesized Pt nanoparticles with different upper potential (a) 0.30 V, (b) 0.60 V, and (c) 1.00 V.

Morphology of the synthesized platinum nanoparticles with different upper potentials of 0.30 V, 0.60 V, and 1.00 V were shown in Fig. 2. From the obtained data, it was known

that $Pt_{0.30V}$ is shaped like parallel leaves, short and small and overlapped each other. The morphological development at $Pt_{0.60V}$ was gradually formed and becoming more visible with the increasing protrude of pointed branches as well as the number of particles. While at $Pt_{1.00V}$ the shaped of the parallel leaves was clearly visible, elongated and there were several branches. These figure demonstrated the different upper potential did affect the particle growth. However, based on previous experiment, nucleation occured in potential range -0.40 V to -2.00 V, while 0.30 V to 0.70 V contributed to the particle growth process [16].

SEM characterization showed the best morphological result is result is $Pt_{0.60V}$ because of the smoother shape and tapered branches resulting in many sites that can increase conductivity [17]. The EDX spectrum shown in Fig. 3 confirmed the platinum nanoparticles formation on the FTO surface. These data indicated the sample has Pt elemental composition which is characterized by the apperance of a signal at 2 to 2.5 keV.

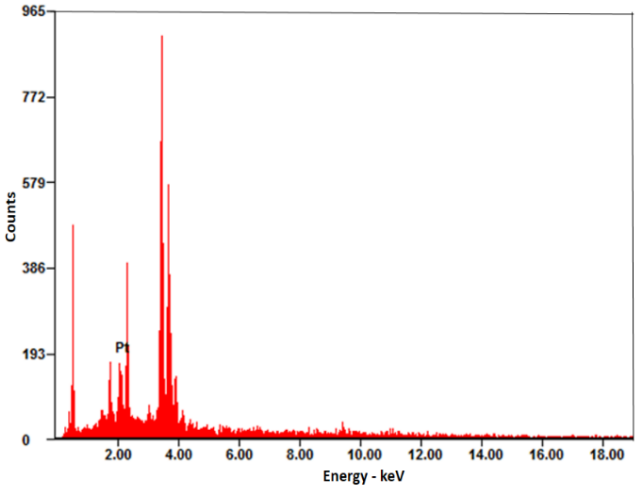

Figure 3. EDX spectrum of platinum nanoparticles deposited above FTO.

In electrochemical processes, electrocatalytic properties are influenced by the electrode. EIS was performed to characterize the properties of synthesized Pt electrocatalyst interface with different upper potentials. Semicircle-shaped of Nyquist plot represented electron transfer resistance and linear shapes represented surface diffusion processes [18]. The smaller R_{ct} (semicircle-shaped) indicated faster electron transfer kinetics. In general, the higher potential during synthesis, the greater R_{ct} [19]. Fig. 4 show Nyquist plot of the synthesized Pt nanoparticles at different upper potentials. It is known that the smallest R_{ct} was produced by $Pt_{0.60V}$, followed by $Pt_{0.30V}$ and $Pt_{1.00V}$. This indicated the highest electron transfer kinetics came from $Pt_{0.60V}$, with longer particle shape such as parallel leaves.

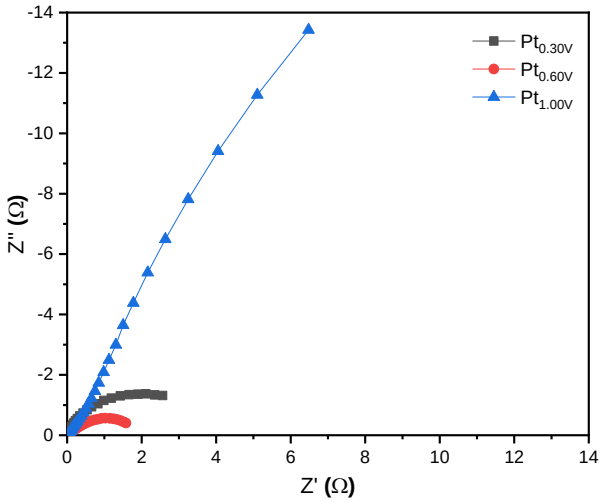

Figure 4. Nyquist plot Pt electrocatalyst with different upper potential.

Then, the ethanol electrooxidation reaction catalytic activity test was evaluated using the CV. The cyclic voltammogram of the Pt electrocatalyst measured in a solution of 1 M ethanol and 0.1 M NaOH as shown in Fig. 5. These results showed the different upper potentials during the sample synthesis process affect the current density. In the forward scan, the ethanol oxidation peak of the three Pt electrocatalyst appeared in the range of -0.60 to -0.30 V. While in the backward scan, three peaks appeared at -0.28 V which was associated with the oxidation of the adsorbed intermediate species. Futhermore, all Pt electocatalysts have reduction peak in the backward scan around -0.10 V associated with Pt oxide reductions. In general, all Pt electrocatalysts showed an oxidation initiation potential at -0.57 V. In short, $Pt_{0.60V}$ has significant oxidation current, indicating the highest catalytic activity when compared to other electrocatalysts.

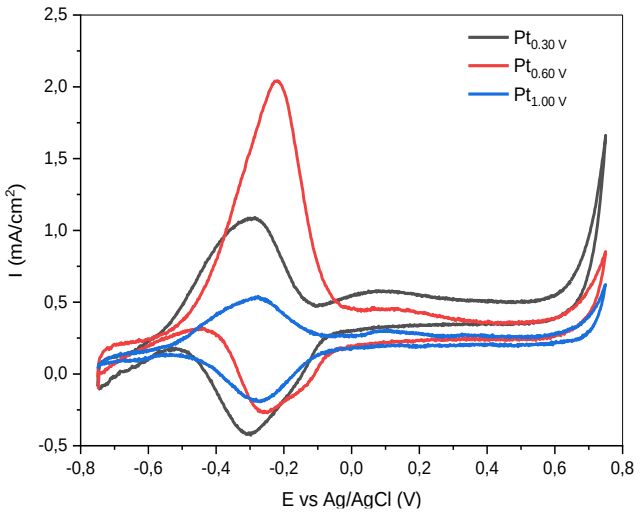

Figure 5. Cyclic voltammogram Pt electrocatalyst in 1 M ethanol and 0.1 M NaOH.

Table 1. The ratio of j_b/j_f Pt electrocatalyst.

Sample	Current Density Forward Scan (j_f)	Current Density Backward Scan (j_b)	Ratio j_b/j_f
$Pt_{0.30V}$	1.16	1.15	0.99
$Pt_{0.60V}$	2.06	1.73	0.83
$Pt_{1.00V}$	0.47	0.48	1.02

The value of current density ratio between forward and backward oxidation peak can determined the tolerance of Pt electrocatalyst to carbonaceous intermediates that was produced during ethanol electrooxidation reactions. The smaller ratio between the backward oxidation peak and forward scan exhibited stronger poisoning-tolerance for the ethanol electrooxidation [20]. Based on data shown in Table 1, $Pt_{0.60V}$ has the lowest j_b/j_f value, followed by $Pt_{0.30V}$ and $Pt_{1.00V}$. Thus, $Pt_{0.60V}$ has the best poisoning-tolerance compared to the other two samples.

4. Conclusion

Pt nanoparticles with parallel leaves and tapered branches shaped was successfully synthesized through square wave pulse deposition by varying the upper potential. $Pt_{0.60V}$ was discovered to have the fastest electron transfer kinetics, higher ethanol electrooxidation current density, low j_b/j_f ratio value that produced the highest poisoning-tolerance and ethanol oxidation activity of the electrocatalysts.

Acknowledgement

The author would like to thank Universitas Negeri Jakarta for funding this research through grant No. 6/PPUI/LPPM/V/2022.

References

[1] J. Tayal, B. Rawat, S. Basu, Bi-metallic and tri-metallic Pt-Sn/C, Pt-Ir/C, Pt-Ir-Sn/C catalysts for electro-oxidation of ethanol in direct ethanol fuel cell, *Int. J. Hydrogen Energy*. **36** (2011) 14884–14897. https://doi.org/10.1016/j.ijhydene.2011.03.035.

[2] L. Yaqoob, T. Noor, N. Iqbal, A comprehensive and critical review of the recent progress in electrocatalysts for the ethanol oxidation reaction, *RSC Adv.* **11** (2021) 16768–16804. https://doi.org/10.1039/D1RA01841H.

[3] Y. Zheng, Advanced Catalytic Materials for Ethanol Oxidation, **10(2)** (2020) 166.

[4] M. Li, A. Kowal, K. Sasaki, N. Marinkovic, D. Su, E. Korach, P. Liu, R.R. Adzic, Ethanol oxidation on the ternary Pt-Rh-SnO_2/C electrocatalysts with varied Pt:Rh:Sn ratios, *Electrochim. Acta*. **55** (2010) 4331–4338. https://doi.org/10.1016/j.electacta.2009.12.071.

[5] U.B. Demirci, Theoretical means for searching bimetallic alloys as anode electrocatalysts for direct liquid-feed fuel cells, *J. Power Sources*. **173** (2007) 11–18. https://doi.org/10.1016/j.jpowsour.2007.04.069.

[6] N.S. Marinkovic, M. Li, R.R. Adzic, Pt-Based Catalysts for Electrochemical Oxidation of Ethanol, Springer International Publishing, 2019. https://doi.org/10.1007/s41061-019-0236-5.

[7] Y.C. Juan Bai, Danye Liu, Jun Yang, A Minireview on Nanocatalysts for Electrocatalytic Oxidation of Ethanol, *ChemSusChem*. **12** (2019) 2117–2132. https://doi.org/10.1002/cssc.201803063.

[8] R.M. Altarawneh, T.M. Brueckner, B. Chen, P.G. Pickup, Product distributions and efficiencies for ethanol oxidation at PtNi octahedra, *J. Power Sources*. **400** (2018) 369–376. https://doi.org/10.1016/j.jpowsour.2018.08.052.

[9] K.M. Hassan, A.A. Hathoot, R. Maher, M. Abdel Azzem, Electrocatalytic oxidation of ethanol at Pd, Pt, Pd/Pt and Pt/Pd nano particles supported on poly 1,8-diaminonaphthalene film in alkaline medium, *RSC Adv.* **8** (2018) 15417–15426. https://doi.org/10.1039/c7ra13694c.

[10] M.A. Shoeib, O.E. Abdelsalam, M.G. Khafagi, R.E. Hammam, Synthesis of Cu2O nanocrystallites and their adsorption and photocatalysis behavior, *Adv. Powder Technol.* **23** (2012) 298–304. https://doi.org/10.1016/j.apt.2011.04.001.

[11] S. Budi, M. Alawiyah, I. Sugihartono, S. Muhab, A.M. Noor, Electrodeposition of AuPt nanoparticles for ethanol electrooxidation application, *AIP Conf. Proc.* **2454** (2022). https://doi.org/https://doi.org/10.1063/5.0078386.

[12] J. Zhang, D. Li, Y. Zhu, M. Chen, M. An, P. Yang, P. Wang, Properties and electrochemical behaviors of AuPt alloys prepared by direct-current electrodeposition for lithium air batteries, *Electrochim. Acta*. **151** (2015) 415–422. https://doi.org/10.1016/j.electacta.2014.11.038.

[13] T.L. Nguyen, V.H. Cao, T. Hai, Y. Pham, T.G. Le, Platinum Nanoflower-Modified Electrode as a Sensitive Sensor for Simultaneous Detection of Lead and Cadmium at Trace Levels, **2019** (2019).

[14] J. Liu, X. Wang, Z. Lin, Y. Cao, Z. Zheng, Z. Zeng, Z. Hu, Shape-controllable pulse electrodeposition of ultrafine platinum nanodendrites for methanol catalytic combustion and the investigation of their local electric field intensification by electrostatic force microscope and finite element method, *Electrochim. Acta*. **136** (2014) 66–74.

https://doi.org/10.1016/j.electacta.2014.05.082.

[15] Y. Zhang, C. Lu, G. Zhao, Z. Wang, Facile synthesis of gold-platinum dendritic nanostructures with enhanced electrocatalytic performance for the methanol oxidation reaction, *RSC Adv.* **6** (2016) 51569–51574. https://doi.org/10.1039/c6ra06370e.

[16] E. Sheridan, J. Hjelm, R.J. Forster, Electrodeposition of gold nanoparticles on fluorine-doped tin oxide: Control of particle density and size distribution, *J. Electroanal. Chem.* **608** (2007) 1–7. https://doi.org/10.1016/j.jelechem.2006.11.015.

[17] N.S.K. Gowthaman, S.A. John, Simultaneous growth of spherical, bipyramidal and wire-like gold nanostructures in solid and solution phases: SERS and electrocatalytic applications, *CrystEngComm*. **19** (2017) 5369–5380. https://doi.org/10.1039/c7ce01044c.

[18] M. Taei, E. Havakeshian, H. Salavati, and F. Abedi, Electrocatalytic oxidation of ethanol on a glassy carbon electrode modified with a gold nanoparticle-coated hydrolyzed CaFe-Cl layered double hydroxide in alkaline medium, *RSC Adv.*, **608** (2016) 27293–27300.

[19] A. Auliya, R. Deswara, M. Paristiowati, S. Budi, Electrodeposition of PANI-NiO as Electrode for Deionization K+ and Cl, *Chem. Mater.* **1** (2022) 1–6.

[20] X. Han, D. Wang, D. Liu, J. Huang, T. You, Synthesis and electrocatalytic activity of Au/Pt bimetallic nanodendrites for ethanol oxidation in alkaline medium, *J. Colloid Interface Sci.* **367** (2012) 342–347. https://doi.org/10.1016/j.jcis.2011.09.087.